

## EVALUATION OF SMOKE DETECTORS FOR USE IN UNDERGROUND MINES

C. D. Litton, NIOSH, Pittsburgh, PA

### ABSTRACT

Laboratory experiments were conducted to determine the responses of a prototype smoke detector and a commercially available photoelectric smoke detector to smoke particles generated from various combustion sources. The prototype smoke detector combines optical scattering measurements with ionization chamber measurements in order to reduce/eliminate nuisance alarms due to the presence of airborne dusts or diesel exhaust particles. The commercially available smoke detector is designed for use in harsh environments where airborne dust represents a major problem due both to nuisance alarms and detector contamination. In the experiments, the responses of the two detectors were measured when exposed to smoke particles from the exhaust of a diesel engine and from a variety of fire sources, including wood, coal, styrene butadiene rubber, and No. 2 diesel fuel. For the solid fuels, data were obtained for both smoldering and flaming combustion. This report describes the experiments, their results, and the use of these results as they apply to early-warning fire sensors capable of the rapid and reliable detection of fires in atmospheres that may or may not be contaminated by either airborne dust or the products produced from diesel engines. Subsequent to these laboratory experiments, six smoke detectors were installed in an underground limestone mine for further testing and evaluation.

**DISCLAIMER:** The findings and conclusions in this report have not been formally disseminated by the National Institute for Occupational Safety and Health and should not be construed to represent any agency determination or policy.

### INTRODUCTION

#### Background

Fire sensors that detect the smoke and gases produced during the early stages of developing fires are often compromised by the presence of background levels of aerosols or gases that mimic the signatures of the developing fires, often resulting in frequent false, or nuisance, sensor alarms. When this frequency is high, the tendency is to either ignore sensor alarms, or to de-energize the sensors, with the potentially catastrophic consequence that an actual fire is not detected. For instance, previous surveys of installed residential smoke detectors (1), indicated that nearly 20% of the detectors did not have functioning power sources, and of these, about one-third were intentionally disconnected because of nuisance alarms. In another study (2), 159 of 273 smoke detectors (59%) examined by fire departments subsequent to the extinguishment of residential fires that went undetected were found to be disconnected from the power source. Nuisance alarms can occur in industrial settings, as well, with similar actions and consequences--real alarms that may be ignored or sensors that are disconnected from their power source--resulting in fires that cost lives and destroy property. A recent workshop (3) highlighted the problems associated with nuisance alarms in aircraft cargo areas and critical telecommunications systems, and stressed the need to develop improved fire sensing systems and test procedures for installed fire detection systems. Fire detection in underground mines and tunnels is often compromised by exhaust products from diesel engines or other vehicles, or by routine procedures, such as welding or flame cutting. In mines, and to a somewhat lesser degree in tunnels, dust is an ever-present problem.

A significant level of research is being conducted to resolve some of these problems. For smoke, efforts continue to more accurately and completely define the properties of smoke produced from different sources (4-7) and to develop improved techniques for smoke measurement (8). Characterizing the signatures of interfering sources using multi-sensor arrays coupled with neural networks or other multi-signature alarm algorithms (9-11) offer promise in many applications. However, the use of these multi-sensor approaches are generally application-specific in that different applications may require different sensors and the necessary algorithms can vary significantly from one application to the next. In some of these approaches, it is not only the relative signals from different sensors, but also the manner in which these signals vary with time, that allow for the discrimination. However, incorporating time into the detection process can delay the alarm and thus be detrimental to the early-warning capability of the system. In underground mines, multi-sensor approaches and simpler gas ratio techniques (12-13) have also been used with varying degrees of success. In general, the use of multi-sensor packages and software to process the signals and make decisions increases both the complexity and the cost of the system, not only in terms of initial expense, but also in terms of system maintenance and sensor replacement.

One alternative to these approaches is the development of simple, stand-alone fire sensors that capitalize on the differences between common, interfering aerosol and/or gas backgrounds and those that result from developing fires so that the discrimination occurs via the sensor and its associated electronics rather than from a more complex processing algorithm. This paper describes the laboratory evaluation of two candidate smoke sensors for the detection of fires in underground mines, where major background sources are dust and the emissions from diesel engines that are used routinely in day-to-day mining operations.

#### The Sensors

The prototype smoke detector utilizes the responses of both an ionization chamber and an optical scattering chamber to discriminate between fires and nuisance sources that are not fire-related. Previous reports (14-16) have described this approach and presented the relevant data using discrete ionization chambers and optical scattering chambers. Briefly, the prototype smoke detector consists of an ionization chamber, typical in design to those used in commercial smoke detectors, where smoke particles are sensed due to the depletion of ions within the air space between two electrodes; and an optical scattering chamber where the collimated light beam from a laser diode is scattered by smoke particles into silicon photo-detectors at forward angles of 15° and 30°. Figure 1 is a schematic of the two chambers. In this study, a prototype instrument was fabricated that combined both chambers into one package, together with improved electronics for storage and processing of the data. A photograph of the fabricated prototype, opened to show the locations of the ionization and scattering chambers, is shown in Figure 2.

The commercial smoke detector is a photoelectric type that measures light scattered at a forward angle of 45°. This detector is designed to operate in harsh environments containing dusts and water mists that can interfere with and degrade the performance of typical smoke detectors. To do this, the detector uses an internal fan that is activated every 35 seconds to sample the surrounding air for a period of five seconds. Within this five second interval, the air is flowed

through a 32  $\mu\text{m}$  filter to remove the dust particles and water droplets that may be present. The air then flows through the scattering chamber where air is sampled for smoke particles before it exhausts to the outside air. Internal sensors detect clogged filters that are easily replaced or signal that the fan is malfunctioning. While this sensor contains no capability to discriminate nuisance particles from smoke particles, it uses flow through a filter to eliminate the dust and it uses light scattering which is relatively insensitive to the very small particles from diesel exhausts, thus reducing the frequency of alarms from these nuisance sources. A schematic of this sensor showing the flow of air and particles during the five second sampling interval is shown in Figure 3. Experiments were conducted to assess the reproducibility of results and the reliability of using either the prototype or commercial sensor for early-warning fire detection.

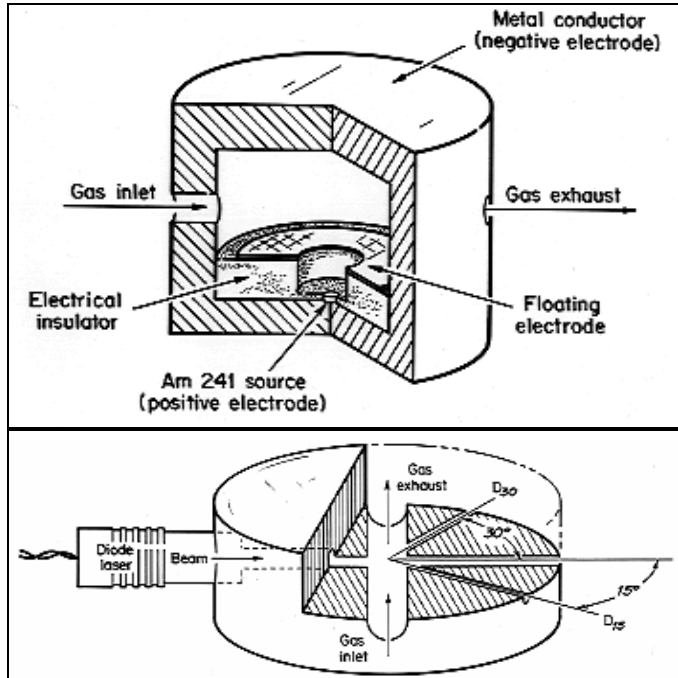


**Figure 1.** Schematic of the ionization chamber (top) and the optical scattering chamber (bottom) used in the prototype detector.

### Experimental

Combustion experiments to produce smoke particles were conducted in the configuration shown in Figure 4 and described in more detail in reference (17). Smoke particles from either flaming or smoldering combustion were generated in a cubical smoke chamber measuring 0.32 m along each edge and then flowed into a standard UL 217 smoke box (18) through a variable-orifice iris that controlled the rate of aerosol accumulation within the smoke box. Inside the smoke box, three of the commercial smoke detectors were placed on a platform and two small internal fans were used to mix the incoming smoke particles to produce a uniform distribution throughout the chamber. The optical density of the aerosol was measured over a 1.48 m optical path using an incandescent lamp and a standard photocell with a peak response at a wavelength of 546 nm and a spectral response matching the spectral response of the human eye. During the experiments, smoke particle samples were continuously extracted through a metal sample port inserted into the top of the smoke box very close to the location of the three commercial sensors and then flowed to three of the prototype smoke detectors. In this configuration, data were obtained for flaming No. 2 diesel fuel (a small pool flame), flaming coal, flaming wood, flaming styrene-butadiene rubber (SBR), smoldering coal, smoldering wood, and smoldering SBR. In a subsequent series of experiments, a Model 8520 DustTrak Aerosol Monitor, using a PM2.5 nozzle, was added to this experimental system along with a six-angle optical scattering module operating at a wavelength of 632.8 nm (see Figure 5 for schematic of the optical scattering device).

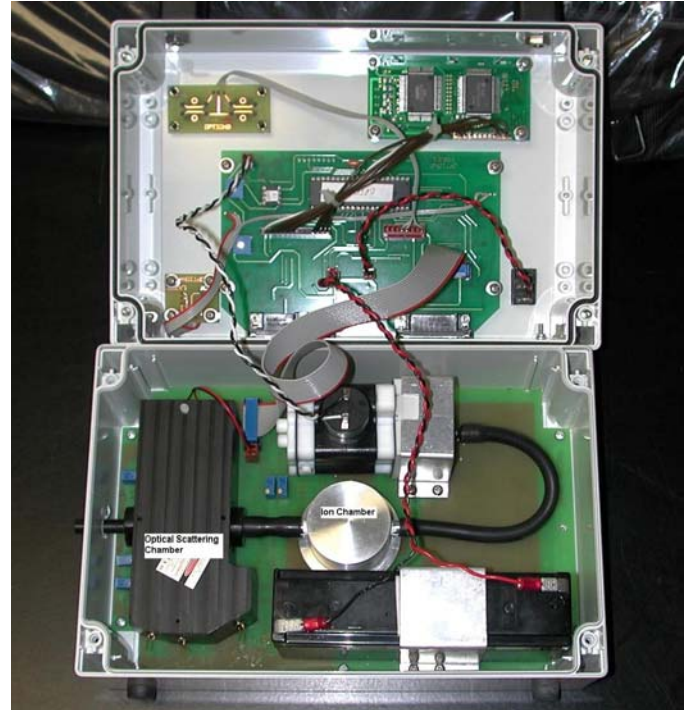


**Figure 2.** Photograph of prototype smoke detector evaluated during this study.

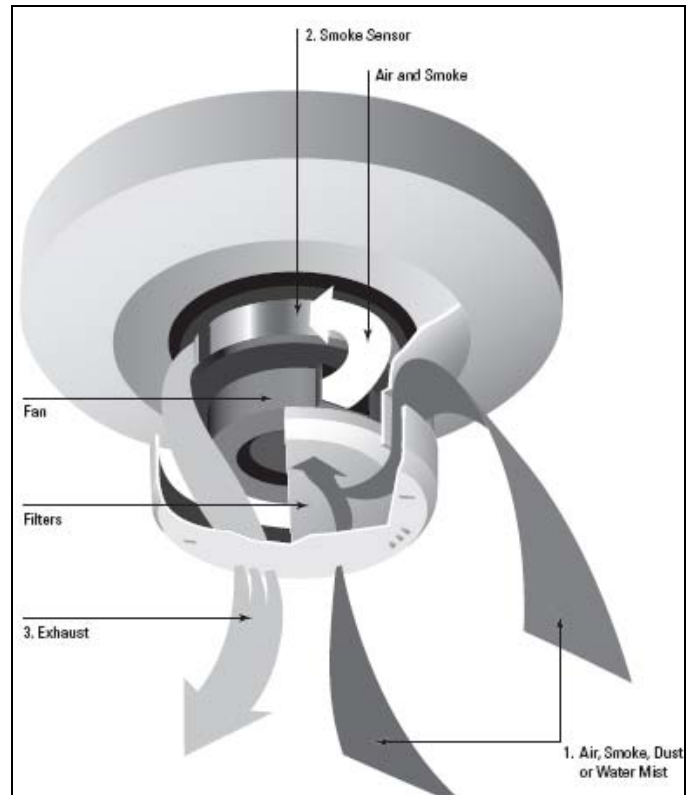


**Figure 3.** Schematic illustrating the flow of air during the five second sampling period of the commercial smoke sensor.

For diesel exhaust particles, the experimental system in which the tests were conducted, known generically as a dust box, is shown in Figure 6 (see Appendix) and described in greater detail in Reference (19). Briefly, dusts or diesel exhaust particles are dispersed near the top of the dust box, allowed to mix thoroughly and then fall via gravity coupled with a small, imposed flow. Samples of diesel exhaust

particles are extracted through 10 mm cyclones near the bottom of the dust box at nominal flow-rates of 2 lpm and flowed to three prototype smoke detectors. In this configuration, data were acquired for particles produced from the exhaust of a diesel generator under different load conditions

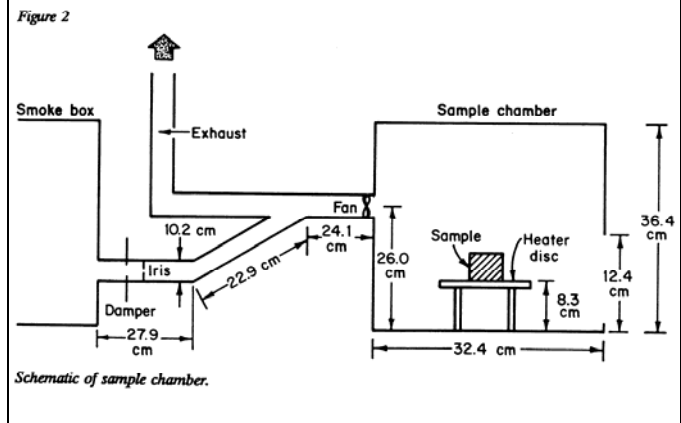
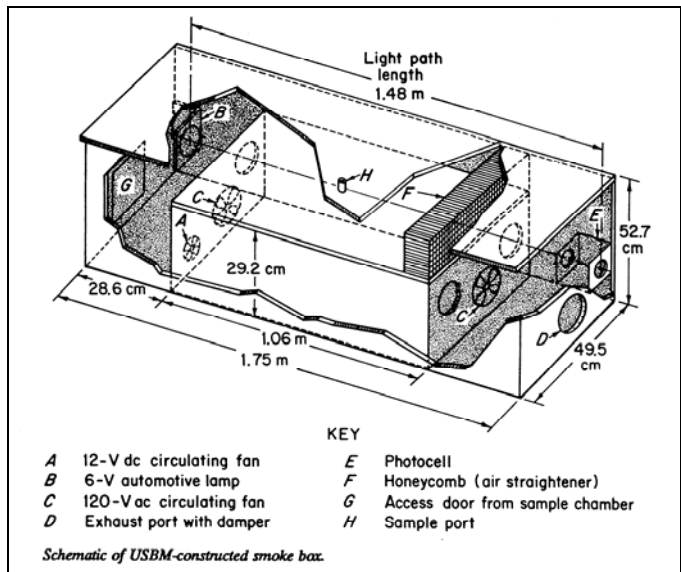


**Figure 4.** Schematic of the smoke box and sample chamber in which the combustion experiments were conducted.

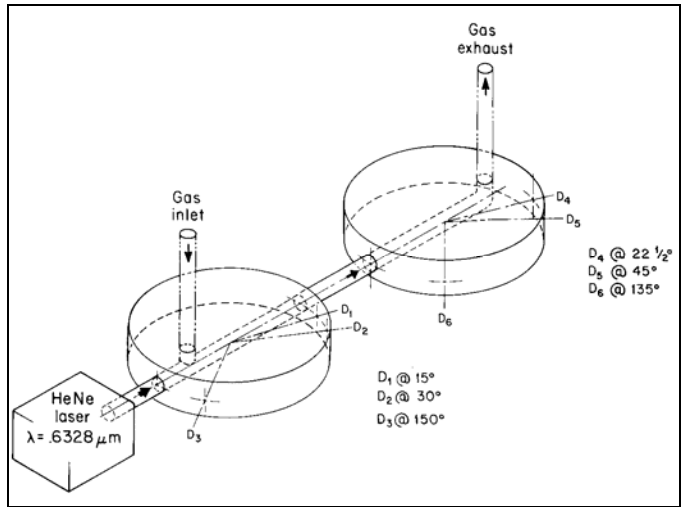


**Figure 5.** Schematic of the six-angle optical scattering device.

During the diesel exhaust experiments, a Tapered Element Oscillating Microbalance (TEOM) (20) was used to continuously measure the mass concentrations of aerosol. In the TEOM, a small filter is mounted onto a hollow tuning fork vibrating at a fixed frequency. Particles in the flow through this filter are deposited on the filter increasing the filter mass. As the filter mass increases, the frequency of vibration decreases proportionally so that the change in mass due to accumulation of particles on the filter is measured as a function of time. The rate of change of the filter mass (due to smoke particles) divided by the volumetric flow rate through the filter yields the average mass concentration.

**RESULTS AND ANALYSIS**

**Experiments Using Only the Prototype Smoke Detector**

Because of their simplicity, the combustion experiments using the UL 217 smoke box could be conducted quickly resulting in a large number of experiments so that several tests under identical conditions could be used to assess the reproducibility of the data and the variations that occurred from one test to the next. In general, combustion aerosol mass concentrations varied over the range from roughly 0.5 mg/m<sup>3</sup> to approximately 30 mg/m<sup>3</sup>. In the data and analysis that follow, particular attention was paid to mass concentrations < 10 mg/m<sup>3</sup>, since it is within this mass concentration range that early-warning fire detectors generally alarm. The basic data acquired for the prototype sensor are summarized as averages in the following Table 1, where the averages represent measurements from typically 2 to 4 tests for each combustion source and combustion mode. It is also worth noting that, although differences for one source or mode, from one test to the next, did occur, these differences were generally within ± 15-20% of the average reported. For each test, the ion chamber and angular scattering signals were found to vary linearly with the well-mixed aerosol mass concentrations in the smoke box. The resultant sensitivities, in volts per mg/m<sup>3</sup>, were defined to be the slopes from linear regressions of the signals as functions of the mass concentrations. In general, the linear regression analyses yielded r<sup>2</sup>-values greater than 0.90 and typically in the range of 0.95 to 0.98. In the table, the response of the ionization chamber is given by the quantity CEV, in volts, corresponding to the change in potential of the floating, collection electrode. The response of the photo-detectors, also in volts, represent the changes in signal at 15° and 30°, V(15) and V(30), respectively. The aerosol mass concentration in the smoke box, M, is in mg/m<sup>3</sup>.

As discussed in a previous paper (14), it is convenient to look at the ratios of the ionization chamber responses to the optical scattering responses as a means for discriminating between fire smoke particles and diesel exhaust particles. These ratios are displayed in Table 2, where the ratio, CEV/V(15), for diesel exhaust particles is more than a factor of ten greater than the average ratio for flaming combustion particles and almost a factor of 35 greater than the average ratio for smoldering combustion particles. It is worth noting at this point that from previous data (21) the response of the ionization chamber to dust particles (typically those in the respirable range from about 0.80 μm to 10 μm) is approximately zero.

When all of the data for both CEV/M and V(15)/M are plotted as a function of the ratio, CEV/V(15), the curves of Figure 7 result, indicating that there are definite correlations. For the ionization chamber, this correlation is given by the expression:

$$CEV/M = 0.02145 [CEV/V(15)]^{2/3} \tag{1}$$

and for the optical scattering at 15°, by the expression:

$$V(15)/M = 0.02145/[CEV/V(15)]^{1/3} \tag{2}$$

A similar correlation (not shown) also exists for the ratio of ionization chamber response to the response of the optical scattering at 30°. These correlations with ratios are important not only because they provide a clear mechanism for determining if the particles are produced from a fire or from a diesel engine but also because they can be used to calculate mass concentrations, surface area concentrations, and average particle diameters as outlined in a

..  
..

previous report (14). Also shown in Figure 7 are the data obtained from previous experiments, labeled FSJ Data (2002).

**Table 1.** Measured sensitivities, volts/(mg/m<sup>3</sup>), for diesel exhaust particles and various combustion aerosols using the bipolar ion chamber with floating collection electrode and the dual angle scattering module at 15° and 30° for the prototype smoke detector. Sensitivities for each combustion source represent the average of 2 to 4 separate experiments.

Aerosol Source	CEV/M	V(15)/M	V(30)/M
Diesel Exhaust	0.455	0.0047	Not Measured
<b>Flaming</b>			
No. 2 Diesel Fuel	0.0778	0.01056	0.0020
Pittsburgh Seam Coal	0.0796	0.0115	0.00267
SBR	0.0934	0.01095	0.0023
Douglas Fir	0.1270	0.00976	0.00136
<b>Smoldering</b>			
Pittsburgh Seam Coal	0.0466	0.0131	0.0041
SBR	0.0426	0.0138	0.0041
Douglas Fir	0.0313	0.0200	0.0051

**Table 2.** Sensitivity ratios for the three types of aerosols measured during these experiments

Aerosol Source	CEV/V(15)	CEV/V(30)
Diesel Exhaust	98.2	Not Measured
Flaming Combustion	9.17	53.0
Smolder Combustion	2.81	9.64

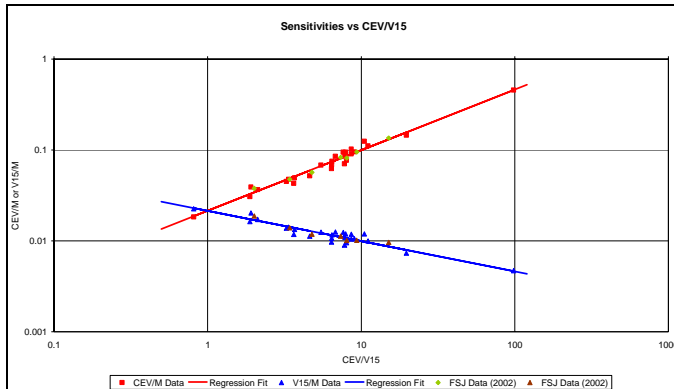


**Figure 7.** Plots of the ionization chamber and 15° optical scattering sensitivities as a function of their ratio for the prototype smoke detector. Also shown are data from previous experiments.

**Experiments Using Both the Prototype and the Commercial Smoke Detector**

Because the commercial smoke detector was not available for the initial experiments conducted using only the prototype smoke detector, a second series of experiments were conducted and simultaneous data acquired for both detectors. This series of experiments used combustion sources and modes identical to those used in the initial series of experiments.

In general, the data for the commercial smoke detector tested indicated that the detector was very responsive to particles from the smoldering combustion mode, not responsive to the diesel exhaust particles, and either not responsive or marginally responsive to particles from the flaming combustion mode. To demonstrate the response of the commercial smoke detector to particles from both the smoldering and flaming modes, Figure 8 is a plot of the response of this sensor to a typical experiment using wood as the combustible sample, along with the responses of the ionization chamber and the 15° optical scattering detector from the prototype smoke detector. The response during the later stages of the flaming wood fire occurred after flaming had ceased and the combustion had returned to a smoldering mode. For data obtained during the flaming combustion mode, the superior response of the ionization chamber is clearly evident. From the data presented in a subsequent section differences in sensor

response are due to the smaller particle diameters generated during the flaming combustion mode compared to the larger particle diameters produced in the smoldering combustion mode.

For all of the data for the smoldering combustion mode, the commercial smoke detector alarmed at an average value of 0.162 volts for the 15° optical scattering signal and an average smoke particle mass concentration of 11.0 mg/m<sup>3</sup>. The average value of the ionization chamber signal at the commercial detector alarm varied from a low value of 0.22 volts to a maximum value of 1.07 volts. The average signals from the 15° angular scattering and ionization chamber at the commercial smoke detector alarm are shown in Table 3. It is worth noting that in the flaming combustion mode experiments the maximum observed mass concentration never exceeded 8.0 mg/m<sup>3</sup>, and it is believed that the combination of these lower mass concentrations coupled with the smaller particle diameters are responsible for commercial smoke detector's poor response to the flaming fires.

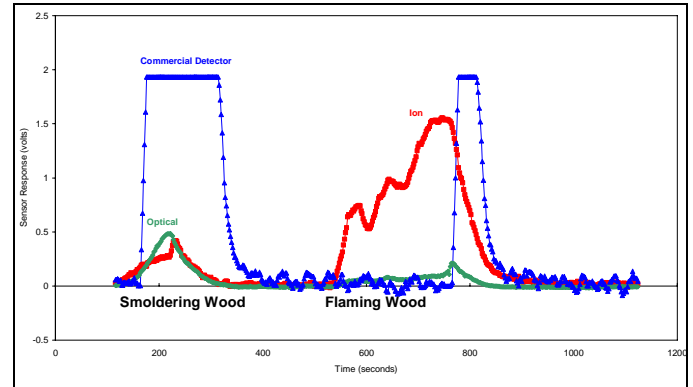


**Figure 8.** Responses of the ion and optical chambers of the prototype smoke detector and the alarms of the commercial smoke detector to both smoldering and flaming wood smoke.

**Table 3.** Average values of the prototype ionization chamber response ( $\Delta$ CEV), the 15° optical scattering response ( $\Delta$ I(15)), and the average smoke particle mass concentrations at the alarm point of the commercial detector to smoldering fires.

Combustible Sample	CEV (volts)	V(15) (volts)	Mass Concentration (mg/m <sup>3</sup> )
Pittsburgh Seam Coal	1.07	0.136	12.6
Douglas Fir	0.28	0.200	8.9
Styrene Butadiene Rubber	0.22	0.182	10.3

**Angular Scattering and Particle Size**

Aerosols produced from combustion processes usually appear in the form of aggregate particles with smaller, primary particles linked together to form irregular shapes that are fractal-like in appearance and amenable to relatively simple analyses to determine their physical characteristics. To determine if the responses of the commercial smoke detector to both flaming and non-flaming fires could be attributed to differences in the particle size and shape of the smoke produced, a subsequent series of experiments were conducted using the six-angle optical scattering device shown in Figure 5, the ionization chamber of the prototype smoke detector, and the Model 8520 DustTrak aerosol monitor operating in the PM2.5 mode. In these experiments, data were analyzed to produce an average dimension for the smoke particle aggregates, the radius of gyration, denoted by  $R_G$ ; the average diameter of the primary particles forming an aggregate,  $d_p$ ; and the relative angular scattering sensitivities, in volts per mg/m<sup>3</sup>. Details of the analysis can be found in References 15 and 21.

For simplicity, data are presented only for experiments for flaming and smoldering Douglas Fir. Figures 9 and 10 show the angular sensitivities for flaming and smoldering Douglas Fir, respectively. Comparing the two figures, it is found that the sensitivity to smoke produced from the smoldering fires is roughly a factor of 2 to 3 greater than the sensitivity to smoke from the flaming fires. This would mean that a much higher flaming smoke concentration would be required for

an angular scattering smoke detector, such as the commercial smoke detector, to alarm at some pre-set voltage—precisely the behavior observed in the previous experiments. In addition, for a given source of particles the relative differences between the angular scattering sensitivities can be used to calculate the values for  $R_G$  and these values coupled with the response of the ionization chamber to yield the primary particle diameters,  $d_p$ . These analyses are shown in Figures 11 and 12 for both flaming and smoldering combustion. From Figure 11, it can be seen that the smoldering case generates particles with a larger radius of gyration than the flaming case. From Figure 12, the primary particle diameters produced from smoldering are also much larger than those produced from flaming. Both the larger primary particle diameters and the larger radii of gyration appear to be major factors that account for the more intense scattering by particles produced from smoldering combustion. Additional analysis similar to that reported previously (22) indicates that the particles produced from smoldering have a much higher volatility and lower carbon content resulting in significantly higher scattering with an albedo that is roughly 1.5 to 2.0 times higher than the albedo from particles produced from flaming combustion.

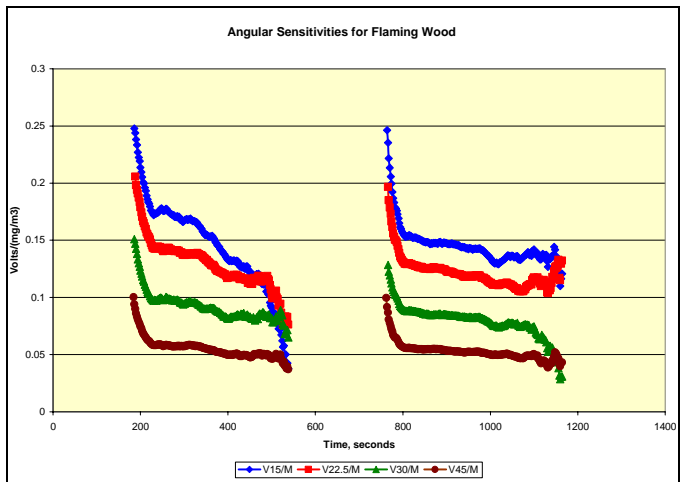


Figure 9. Angular sensitivities to smoke from flaming Douglas Fir.

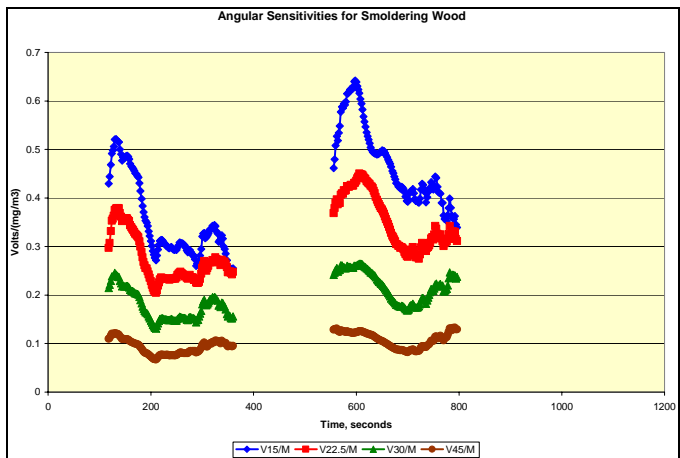


Figure 10. Angular sensitivities to smoke from smoldering Douglas Fir.

**In-Mine Installation**

In October 2007, six of the commercial smoke detectors were installed in an underground limestone mine. This particular mine is relatively young and the underground workings relatively compact, so that the underground areas to be protected are all relatively close to each other. The six detectors were located according to the diagram of Figure 13 and connected to a central control pane, shown in Figure 14, which was located in the electrical room. The outputs of the detectors were monitored continuously and any alarms or malfunctions

recorded by the control panel software, which then reset the detectors automatically. To-date, the system has recorded one detector alert due to clogging of the inlet filter on the detector. Not long after the initial installation, the main electrical line connecting four of the smoke detectors to the central control panel was severed by mining equipment resulting in the loss of 4 of the 6 detectors. However, the remaining two sensors continued to function properly without any alarms or malfunctions.

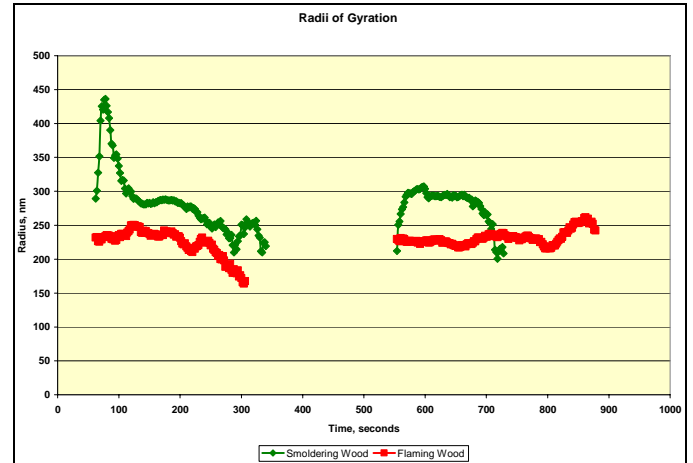


Figure 11. The radii of gyration,  $R_G$ , for both smoldering and flaming Douglas Fir.

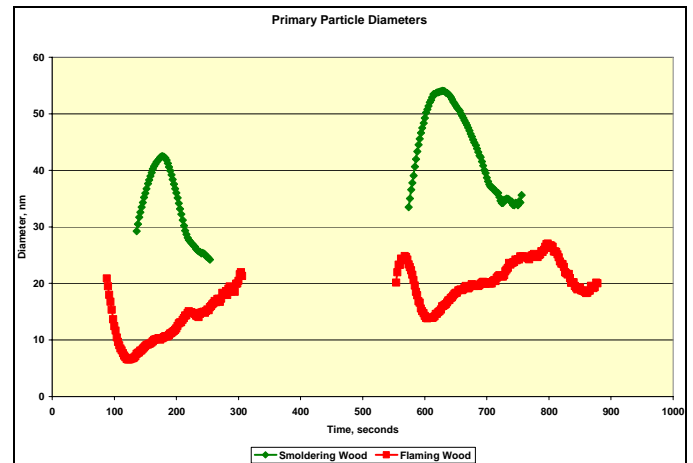


Figure 12. Primary particle diameters for smoldering and flaming Douglas Fir.

Approximately two months following the initial installation, the severed line was repaired and the system restored to operation only to have the line severed approximately one day later. A subsequent visit found that the central control panel had been rendered inoperative due to penetration by massive quantities of dust. The control panel was returned to the Pittsburgh Laboratory, refurbished with improved seals to reduce dust penetration, and then re-deployed in the mine. The system has now remained operational for ~3 months without any major problems or malfunctions. The numbers of alarms or system warnings will be collected and analyzed during the next visit and it is expected that the system will remain installed throughout the upcoming year and upgraded with the addition of 4 to 6 additional smoke detectors.

**CONCLUSIONS**

The results of this study indicate that the prototype smoke detector fabricated to combine both the ionization chamber and the optical scattering chamber functions as expected. The responses of the two components are similar to the responses previously measured as separate components. The utilization of the ratio of ionization chamber signal to optical scattering signal shows potential for use in

the discrimination of very fine particles, such as those from diesel exhausts, and very coarse particles, such as mine dusts. The commercial smoke detector showed adequate response to smoldering combustion, but did not exhibit good response to flaming fires. However, the potential for the detector to be insensitive to very small particles, such as those from diesel exhausts and flaming fires, because it operates on the principle of light scattering warrants further test and evaluation under typical mine conditions. In addition, the lifetimes of the filters used in the commercial smoke detectors need further evaluation for their adequacy. The in-mine evaluation of the smoke detection system is expected to continue for at least another year.

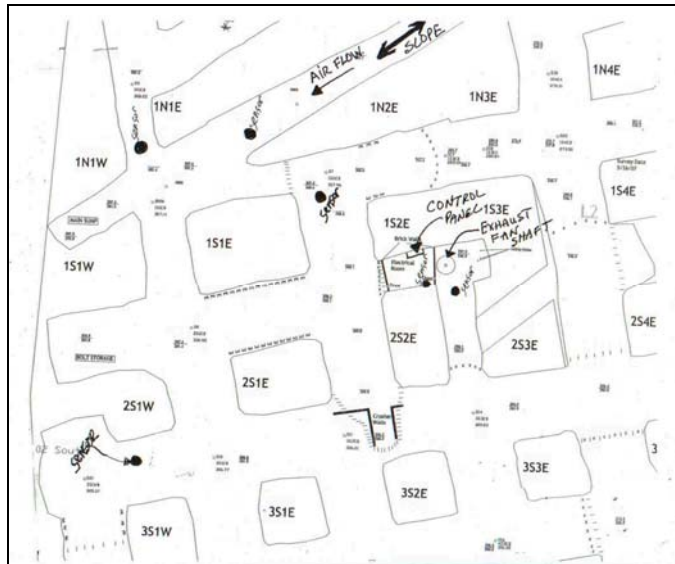


**Figure 13.** Diagram showing the location of smoke detectors in the underground limestone mine. Air flows down the slope and is exhausted through the exhaust fan shaft. Intervening flow patterns are ill-defined.

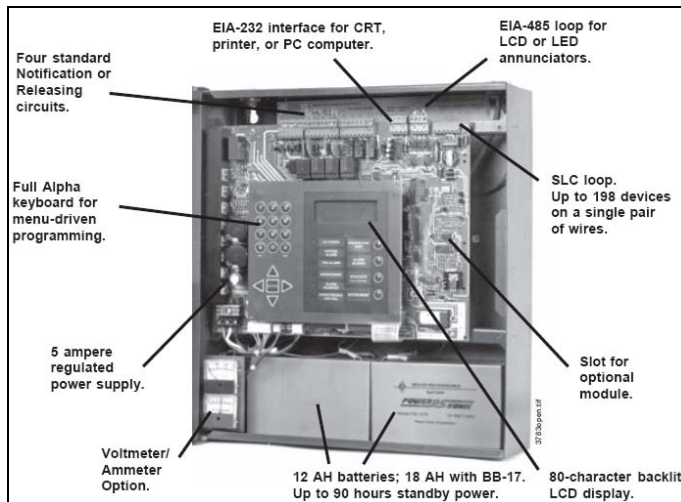


**Figure 14.** Photograph of the central control panel used for the in-mine installation of smoke detectors. The control panel measures 16 1/8" x 14 1/2" x 5 1/2" and can accommodate up to 99 individual smoke detectors.

#### REFERENCES

1. Smith, C.L., (1994), "Smoke Detector Operability Survey," *Report on Findings*, U.S. Consumer Product Safety Commission, October, 98 pp.
2. Smith, L.E. (1995), *Fire Incident Study. National Smoke Detector Project*, U. S. Consumer Product Safety Commission, January, 61

pp.

3. Grosshandler, W.L. (Editor), (1998), "Nuisance Alarms in Aircraft Cargo Areas and Critical Telecommunications Systems," *Proceedings of the Third NIST Fire Detector Workshop*, NISTIR 6146, BFRL, NIST, 34 pp.
4. Mulholland, G.W. and C. Croarkin, (2000), "Specific Extinction Coefficient of Flame Generated Smoke," *Fire and Materials* 24(5):227-230, September/October.
5. Choi, M.Y., Mulholland, G.W., Hamins, A. and Kashiwagi, T., (1994), "Experimental Study of the Optical Properties of Soot and Smoke," *NISTIT 5499, NIST, Annual Conference on Fire Research: Book of Abstracts*, October, pp. 123-124.
6. Sorensen, C.M. and G.D. Feke, (1995), "Post-Flame Soot," *Proceedings of the International Conference on Fire Research and Engineering (ICFRE)*, pp. 281-285.
7. Smoke Characterization Project, (2007), Final Report, Project Number: 06CA08584, File Number: NC 5756, Underwriters Laboratories Inc., Northbrook, IL 60062, April 24, 2007.
8. Mulholland, G.W., E.L. Johnsson, D.A. Shear, and M.G. Fernandez, (1998), "Design and Testing of a New Smoke Concentration Meter," *Proceedings of the Fall Conference. Fire Retardant Chemicals Association (FRCA)*, pp. 41-49.
9. Gottuk, D.T., M.J. Peatross, R.J. Roby and C.L. Beyler, (1999), "Advanced Fire Detection Using Multi-Signature Alarm Algorithms," *Proceedings of the International Conference on Automatic Fire Detection "AUBE 99"*, pp. 237-246.
10. Milke, J.A., (1995), "Application of Neural Networks for Discriminating Fire Detectors," *Proceedings of the International Conference on Automatic Fire Detection AAUBE >95"*, pp. 213-222.
11. Grosshandler, W.L., (1995), "Review of Measurements and Candidate Signatures for Early Fire Detection," NISTIR 5555, BFRL, NIST, 36 pp.
12. Brinn, M. and B. Bott, (1994), "A Fresh Approach to Mine Fire Detection," *Transactions of the Institute of Mining Engineers*, pp. 71-74.
13. Litton, C.D., R.S. Conti, J.G. Tabacchi, and R. Grace, (1993), "Evaluation of a Nitric Oxide-Compensated Carbon Monoxide Fire Sensor," *BuMines IC 9339*, 10 pp.
14. Litton, C.D., (2002), "The Use of Light Scattering and Ion Chamber Responses for the Detection of Fires in Diesel Contaminated Atmospheres," *Fire Safety Journal*, vol. 27, pp. 409-425.
15. Litton, C.D., K.R. Smith, R. Edwards and T. Allen, (2004), "Combined Optical and Ionization Measurement Techniques for Inexpensive Characterization of Micrometer and Submicrometer Aerosols," *Aerosol Science and Technology* 38(1):1054-1062.
16. Edwards, R., K.R. Smith, B. Kirby, T. Allen, C.D. Litton and S. Hering, (2006), "An Inexpensive Dual-Chamber Particle Monitor: Laboratory Characterization," *J. Air & Waste Manage. Assoc.*, 56(6):789-799.
17. UL 217- Single and Multiple Station Smoke Alarms. Underwriters Laboratories Inc., Northbrook, IL, 60062.
18. Edwards, J.C. and G.S. Morrow, (1995), "Development of Coal Combustion Sensitivity Tests for Smoke Detectors," *U.S. Bureau of Mines Report of Investigations 9551*, 12 pp.
19. Marple, V.A. and K.L. Rubow, (1983), "An Aerosol Chamber for Instrument Evaluation and Calibration," *Am. Ind. Hyg. Assoc. J.*,

44:361-367.

20. Patashnick, H. and G. Rupprecht, (1986), "Microweighing Goes On-Line in Real Time," *Research and Development*, 28(6):74-78.
21. Litton, C.D., (2002), "Studies of the Measurement of Respirable Coal Dusts and Diesel Particulate Matter," *Measurement Science*

*and Technology*, 13:365-374.

22. Litton, C.D., (1997), "Fractal Properties of Smoke Produced from Smoldering and Flaming Fires," *Proceedings of Symposium on Combustion, Fire and Explosion, and Alternative Fuels, ASME International Mechanical Engineering Congress and Exposition*, Dallas, TX, Nov. 16-21.

## APPENDIX

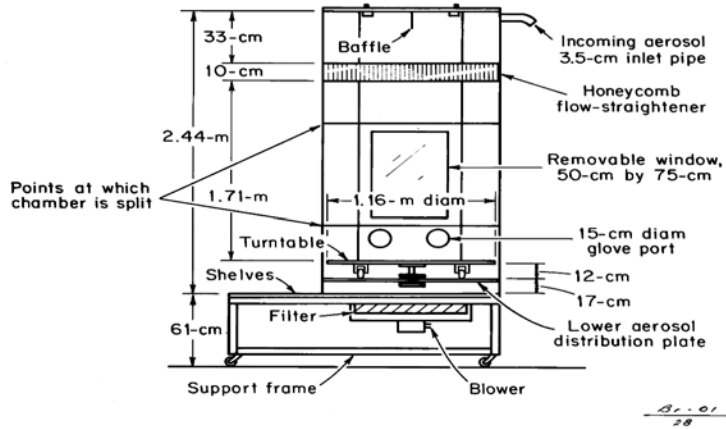


**Figure 6.** Schematic (A) and photograph (B) of the dust box where the response to diesel exhaust particles was measured.